*International Journal of Astrobiology* 10 (3): 161–175 (2011)
doi:10.1017/S1473550411000048 


# Concretions in exhumed and inverted channels near Hanksville Utah: implications for Mars

Jonathan D. A. Clarke[1,2] and Carol R. Stoker[3]

[1]*Mars Society Australia, c/o 43 Michell St Monash, ACT 2904, Australia*
[2]*Australian Centre for Astrobiology, Ground Floor, Biological Sciences Building, Sydney, NSW, Australia*
*e-mail: jon.clarke@bigpond.com*
[3]*NASA Ames Research Center, Moffett Field, CA 94035, USA*

**Abstract**: The landscape near Hanksville, Utah, contains a diversity of Mars analogue features. These included segmented and inverted anastomosing palaeochannels exhumed from the Late Jurassic Brushy Basin Member of the Morrison Formation that hosts abundant small carbonate concretions. The exhumed and inverted channels closely resemble many seen on the surface of Mars in satellite imagery and which may be visited by surface missions in the near future. The channels contain a wealth of palaeoenvironmental information and are potentially of astrobiological interest, but intrinsically difficult terrain would make their study challenging on Mars. We show that an un-exhumed channel feature can be detected geophysically, and this may allow their study in more easily accessed terrain. The concretion's morphology and surface expression parallel the haematite 'blue berries' that are strewn across the surface of Meridiani Planum on Mars. They are best developed in poorly cemented medium to coarse channel sandstones and appear to have formed during deep burial.

*Received 17 December 2010, accepted 24 January 2011, first published online 25 February 2011*

**Key words:** Mars regolith, geomorphology, relief inversion, palaeochannels, concretions.

## Introduction

Satellite images of Mars have revealed numerous fluvial channels dating from the Late Noachian through to Early Hesperian (Howard *et al.* 2005; Irwin *et al.* 2005; Mangold *et al.* 2008; Burr *et al.* 2009; Newsome *et al.* 2010), many of which have been exhumed and inverted through denudation (Pain *et al.* 2007; Williams *et al.* 2009). Relief inversion is common on Earth during landscape evolution and many examples are known (Pain & Ollier 1995). Properly interpreted, such features provide insight into the Martian water cycle, fluvial hydrology and processes and rates of landscape evolution. Examples of such features have been considered as landing sites for future unmanned Mars missions such as the *Curiosity* Mars Science Rover (Marzo *et al.* 2009, Rice & Bell 2010).

Images from Mars Exploration Rover *Opportunity* have revealed a widespread unit of sandy lacustrine and Aeolian evaporitic sediments containing haematite concretions (Klingelhofer *et al.* 2004; McLennan *et al.* 2005; Sefton-Nash & Catling 2008) formed during diagenesis and now being concentrated by Aeolian deflation into a lag of wind-rippled sand (Soderblom *et al.* 2004). Haematite concretions have been reported from terrestrial Aeolian sandstones and acidic salt lakes and have been used as Mars analogues (Chan *et al.* 2004; Morris *et al.* 2005; Benison & Bowen 2006; Benison *et al.* 2007). Elsewhere on Mars sulfates (McLennan *et al.* 2005) and carbonates (Morris *et al.* 2010) are present as secondary precipitates formed during alteration and diagenesis. Such features provide insight into the subsurface physical and chemical aqueous environment during their formation.

In this paper, we describe a new location that provides an analogue to exhumed and inverted Martian channels and for concretions located on the edge of the Colorado Plateau in Utah. We will characterize these features and document their geologic and geomorphic context and describe their significance compared to similar, previously documented occurrences of inverted and exhumed relief and concretions. Lastly, we will argue that this study provides a good analogue for the level of investigation that can be achieved with a human surface mission on Mars.

## Mars Desert Research Station (MDRS) and Morrison Formation geologic setting

The study area is located near Hanksville, Utah, on the edge of the San Rafael swell (Fig. 1). The site is the location of the MDRS (Persaud *et al.* 2004), a facility established by the Mars Society for analogue research in the disciplines of engineering, planetary science, astrobiology and human factors, and as a platform for education and outreach programmes. Our investigations are part of a multi-disciplinary field programme carried out at MDRS in 2009–2010 (Foing *et al.* 2011, Stoker *et al.* 2011) and reported elsewhere in this issue.

The region (Western Regional Climate Center 2010) has an arid climate, over a 56-year period (1948–2005), Hanksville

Table 1. *Stratigraphy of the Jurassic and Cretaceous near Hanksville*

| Age | Group | Formation | Member | Thickness (m) |
|---|---|---|---|---|
| Cretaceous | Mesa Verde | | | 300 + |
| | | Mancos Shale | Musak Shale | 600–800 |
| | | | Emery Sandstone | 250 |
| | | | Blue Gate Shale | 1400 |
| | | | Ferron Sandstone | 250 |
| | | | Tununk Shale | 575 |
| | | Dakota Sandstone | | 0–50 |
| | | Cedar Mountain | | 0–125 |
| Jurassic | | Morrison Formation | Brushy Basin | 60–225 |
| | | | Salt Wash | 30–235 |
| | San Rafael Group | Summerville | | 200 |
| | | Curtis | | 0–80 |
| | | Entrada | | 475–780 |
| | | Carmel | | 310–99 |
| | Glen Canyon Group | Navajo Sandstone | | 800–1100 |
| Triassic | | Kayeata | | 350 |
| | | Wingate Sandstone | | 320–370 |

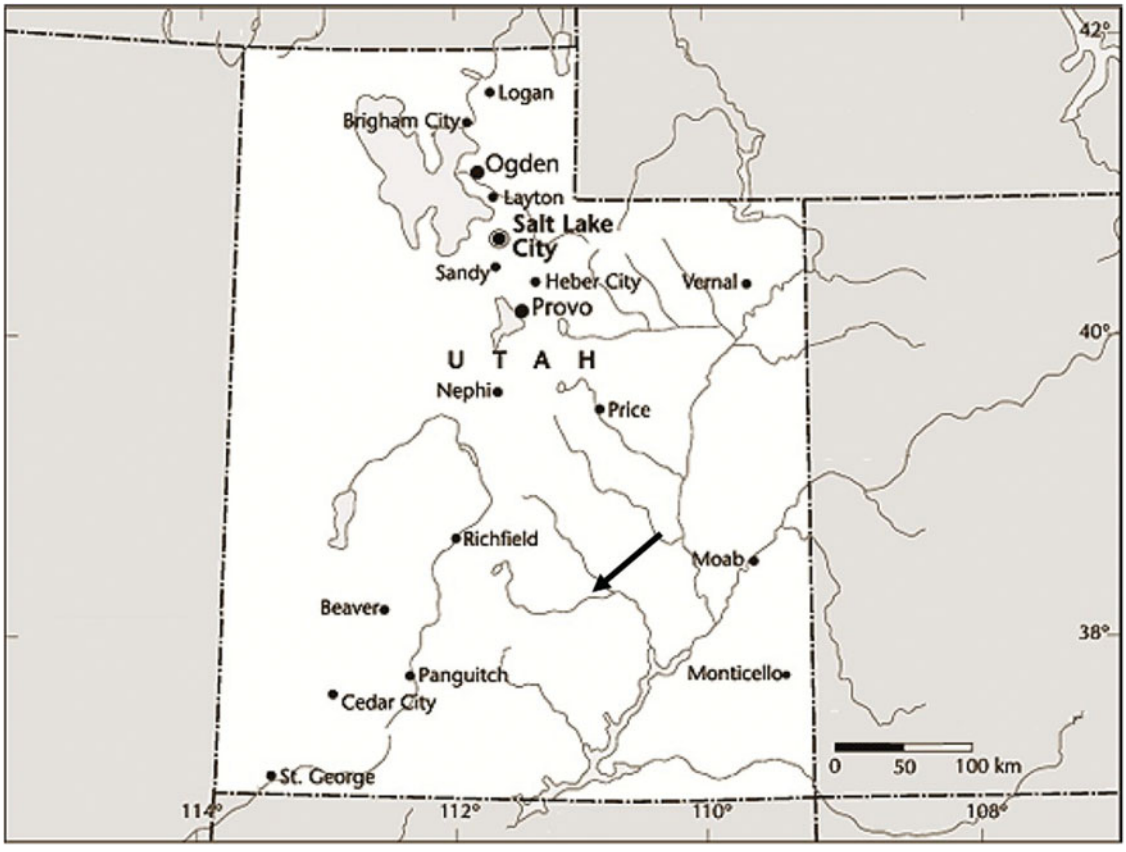


**Fig. 1.** Map showing location of study area in Utah (arrowed).

received an annual average precipitation of 141.22 mm, of this 14.73 mm (10.4%) occurred as snow. Precipitation was highest during August–October. The hottest month was July, with an average daily maximum temperature of 37.1 °C and a daily minimum temperature of 16.3 °C. The coldest month was January, with an average daily maximum temperature of 5.2 °C and a minimum temperature of −10.9 °C. Monthly minima are below freezing from November to March. The study area lies between the altitudes of 1340 and 1400 m.

The stratigraphy of the area (Table 1) consists of a dissected succession of near flat-lying Cretaceous and Jurassic sandstones and shales. The main unit studied is the Jurassic Morrison Formation, in particular the uppermost Brushy Basin Member (Hintze & Kowallis 2009).

https://doi.org/10.1017/S1473550411000048 Published online by Cambridge University Press

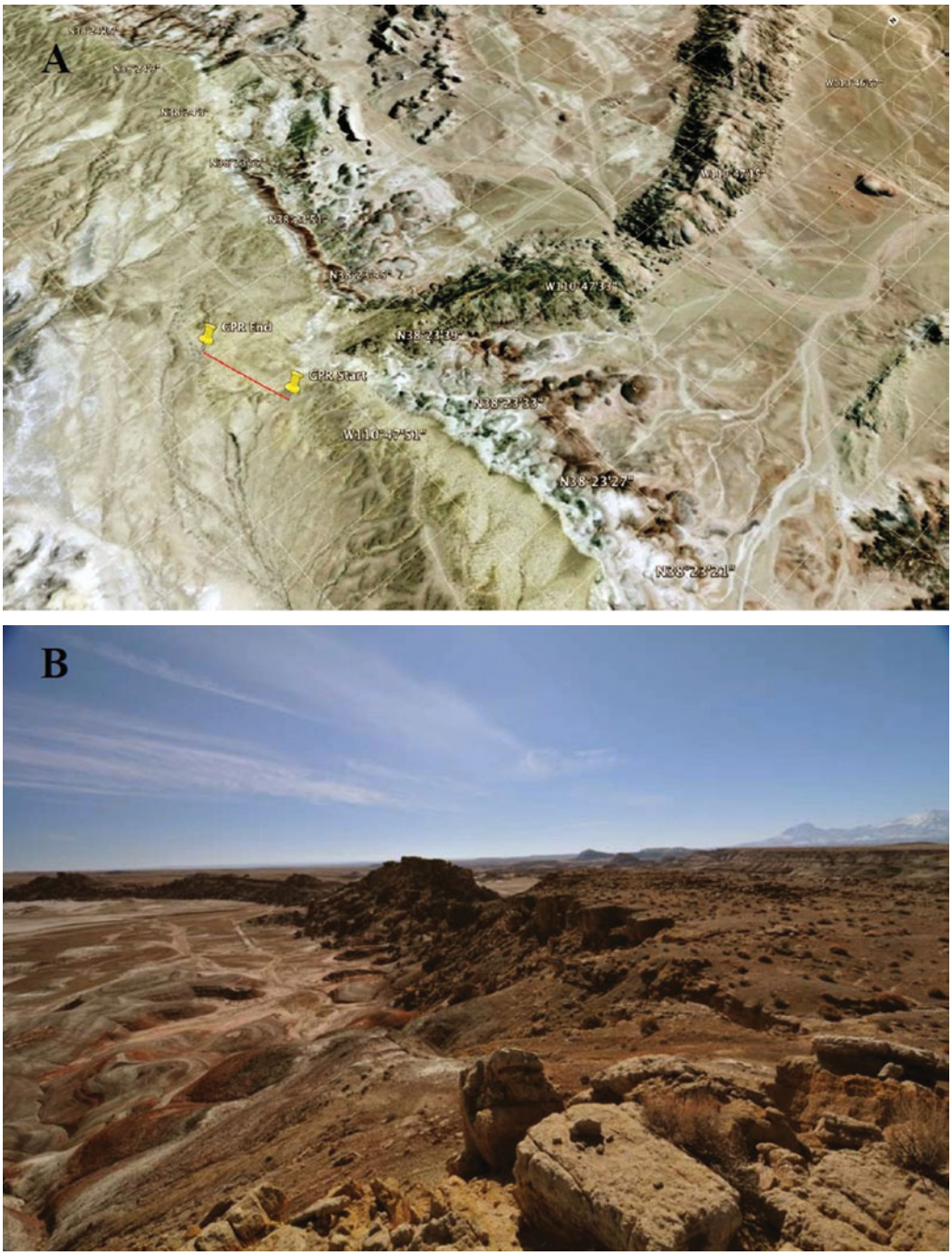


**Fig. 2.** (a) Oblique Google Earth imaging showing western end of 'Kissing Camel Ridge' formed by exhumation of a fluvial channel within the Brushy Basin member of the Morrison Formation and the position of GPR traverses along interpolated un-exhumed extension of the channel. (b) View east along Kissing Camel Ridge from the western end.

The landscape consists of mesas and scarp-bounded surfaces resulting from erosion of the flat-lying succession of alternating units of greater and lesser resistance to erosion. Clay-rich units being more easily eroded and sandstones are less. The sandstone surfaces form smooth plains and the clay-rich materials mostly dissected slopes. In the immediate vicinity of MDRS, the Brushy Basin Member forms a dissected plain of cracking clays (Clarke & Pain 2004). Fluvial channels are exposed on the steep slopes or are being exhumed as inverted relief. It is these features that we put forward as new Mars analogues.

## Methods

Study methods consisted of air photo interpretation, geological documentation of the inverted and exhumed channels and the concretions associated with them, ground-penetrating radar surveys of the best exposed and most accessible example

https://doi.org/10.1017/S1473550411000048 Published online by Cambridge University Press

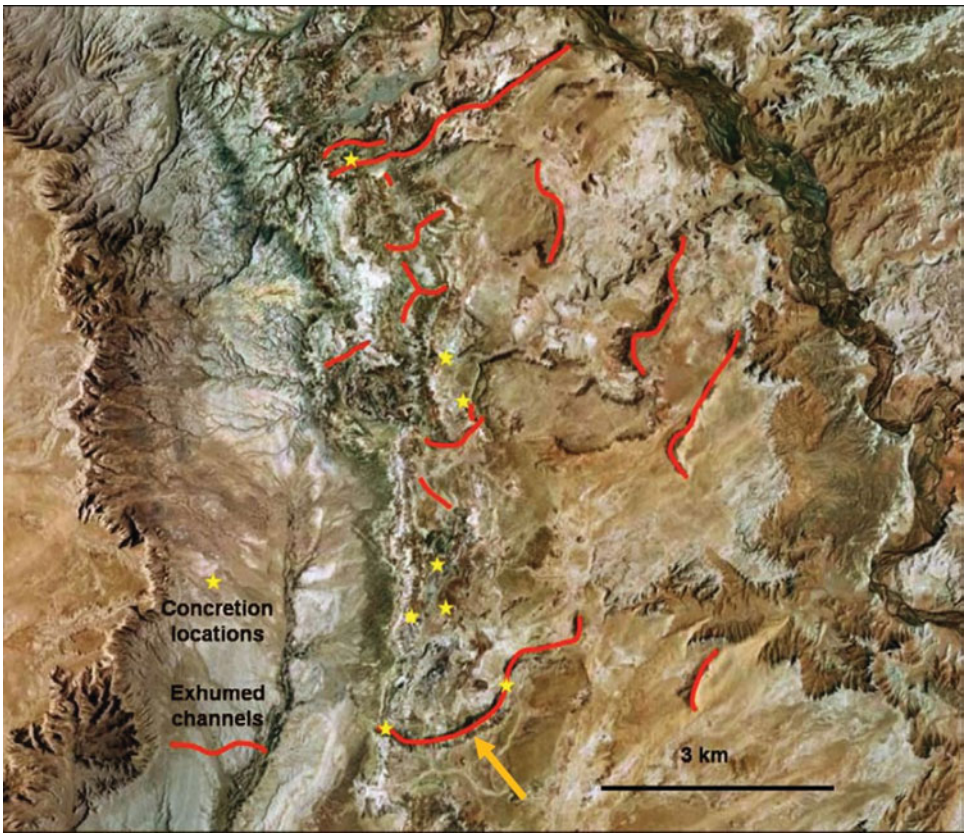


**Fig. 3.** North–east flowing exhumed and inverted anastomosed palaeochannels in the study area with sample concretion locations marked. Flow direction is to the northeast. KCR arrowed.

of a partially exhumed channel, and sampling of outcrops by hand and using a Shaw Backpack Drill. In the laboratory, samples were analysed for mineralogy using XRD with a TERRA field-portable XRF/XRD (In Xitu Inc.; Sarrazin *et al.* 2005) and cross checked using a Portable Infra-Red Mineral Analyser or PIMA (Thomas & Walter 2002). The PIMA II, manufactured by Integrated Spectronics, works in the short wavelength infrared, and has 601 contiguous spectral bands between 1300 and 2500 nm. The PIMA detects minerals containing $OH^{-}$, $H_2O$, $CO_3^{3-}$, $PO_4^{2-}$ and $SO_4^{2-}$. Mineral identification by spectral matching is automated and takes about a minute per sample. The instrument can be used in either the field or in the laboratory. Thin sections of concretionary units were half-stained with Alazarin Red and Potassium ferrocyanin to show their carbonate mineralogy and then examined using a polarizing transmitted light microscope.

### *Exhumed channel observations*

Fluvial channels are composed of more permeable sediments such as sands and gravels than their floodplains or valley sides that are more likely composed of silts and clays. Their greater permeability results in high rates of fluid flow and greater likelihood of cementation compared to their flanking materials. Lowering of the landscape through denudation processes such as mass wasting, fluvial dissection or Aeolian deflation will exhume the channels, leaving the more indurated examples as ridges in the landscape, inverting the former topography (Pain & Ollier 1995). In the study area, Jurassic palaeochannels in the Brushy Basin Member has been exhumed in this manner, leaving numerous segmented sinuous ridges. The resistant sandstones and conglomerates of the channels form cap rocks that protect the underlying floodplain clays from erosion. Eventually the cap rocks are removed by scarp retreat, leaving isolated boulders, the clay ridge then being vulnerable to erosion.

The best developed and most accessible examples of these channels (Fig. 2) have been given the informal name of 'Kissing Camel Ridge' (KCR) by previous people who have worked in the area, possibly due to the rock formations on its crest. The channel that forms the ridge is partly exhumed from the surrounding floodplain shales, allowing its buried component to be explored using geophysics.

## Fluvial facies

The Brushy Basin Member of the Late Jurassic Morrison Formation was deposited in a foreland basin setting draining highlands to the west and a marginal to enclosed evaporitic basin to the east. The depositional climate was arid to semi-arid environment (Demko & Parish 2001; Demko *et al.* 2004). In the study area, palaeocurrents indicate flows in a generally north-easterly direction (Fig. 3). The sediments contain a major contribution of weathered volcanic ash, expressed as

https://doi.org/10.1017/S1473550411000048 Published online by Cambridge University Press

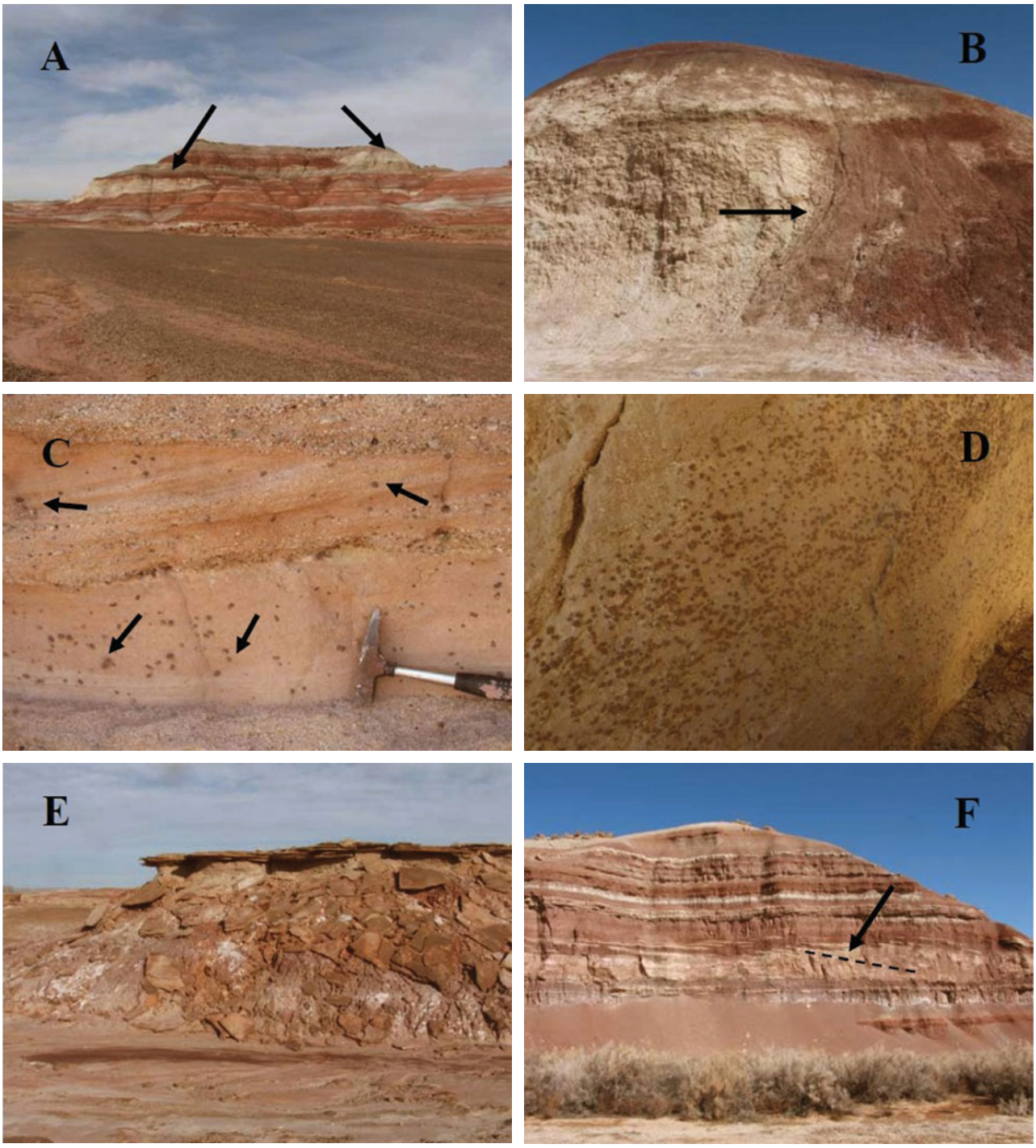


**Fig. 4.** (a) Two channels (arrowed), part of anastomosing channel complex channels ~100 m wide. (b) Edge of channel unit ~5 m thick (arrowed) exposed on side of rise. (c) Concretions (some arrowed) in pebbly sandstone. (d) Cluster of brown-weathered in channel sandstone. (e) Thinly bedded laminated sandstone of crevasse splay facies. (f) Lateral accretion surfaces of meandering channel facies (arrowed and outlined).

residual glass shards, bentonite beds and abundant smectites in the floodplain facies.

Deposition was dominated by anastomosing fixed fluvial channels (Miall & Turner-Peterson 1989; Kjemperud *et al.* 2008). Sand and gravel channels 20–100 m wide and 2–15 m thick, composed of cross-bedded sandstone, are embedded in floodplain deposits of shale (Fig. 4). The fixed channels are possibly the result of both gallery vegetation and very cohesive banks rich in smectic clays from the weathering of volcanic ash (bentonites). Adjacent to the channels are levee bank deposits of fine sands and siltstone showing planar to ripple lamination (Fig. 4). Interbedded with the floodplain shales are thin (<1 m) lenticular to laterally extensive sand and sandstone beds generally white in colour (Figs 6 and 8). These are interpreted as crevasse splay deposits. The beds have erosional to planar bases and are either massive or parallel laminated. Palaeosols

https://doi.org/10.1017/S1473550411000048 Published online by Cambridge University Press

Table 2. *Sandstone petrography, based on grain counts*

| Sample | Quartz | Feldspar | Clay pellets | Amphibole | Total |
|---|---|---|---|---|---|
| 215<br>56 grains | Vein 82.1%<br>Metamorphic 3.6%<br>Chert 5%<br>Total 91.1% | Plag 3.6%<br>Total 3.6% | 3.6% | 1.8% | 100.1% |
| 457<br>142 grains | Vein 85.9%<br>Metamorphic 0.7%<br>Chert 8.9%<br>Total 95.5% | k-spar 1.4%<br>Total 1.4% | 2.8% | | 99.7% |
| 463<br>297 grains | Vein 85.8%<br>Metamorphic 1.7%<br>Chert 9.3%<br>Volcanic 0.7%<br>Total 97.3% | k-spar 2.0%<br>Plag 0.3%<br>Total 2.4% | 0.3% | | 100% |
| Average<br>495 grains | Vein 85.5%<br>Metamorphic 1.6%<br>Chert 8.7%<br>Volcanic 0.4<br>Total – 96.2% | k-spar 1.6%<br>Plag 0.6%<br>Total 2.2% | 1.1% | Trace | 99.5% |

Slight discrepancies in numbers are due to rounding.

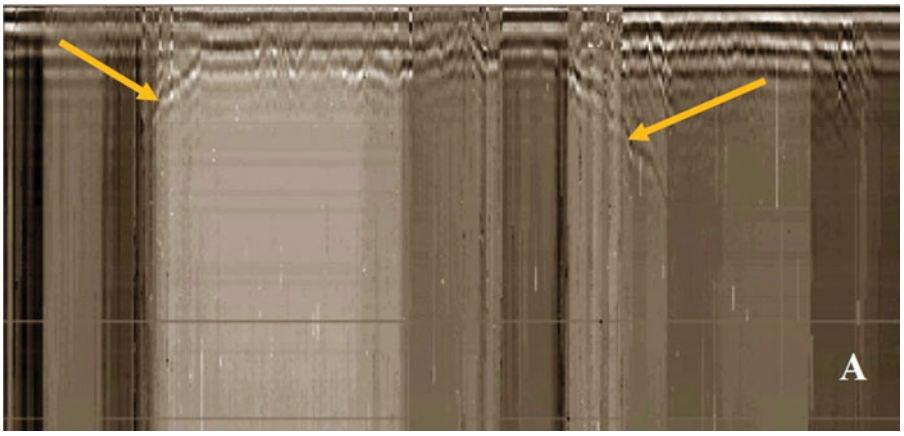


**Fig. 5.** A GPR traverse to west of KCR with edges of channel arrowed.

are common, recognized by prominent brown and white mottling and root impressions (see Demko *et al.* 2004 for further detail).

Meandering river channels are a minor architectural theme of the Brushy Basin Member of the Morrison Formation. The meandering channels are typically thin (<2 m) and are laterally extensive (100–200 m in width). Apart from the overall thinness of individual units and width to thickness ratios of ~100:1, meandering channel units are generally characterized by lateral accretion surfaces visible in the best outcrops, sometimes mirrored lateral accretion surfaces are visible as the cliff face cuts across a bend. Some published descriptions of these facies can be found in Miall & Peterson (1989).

In the Hanksville area, floodplain clays in the Brushy Basin Member are only weakly indurated to form shales. Sandstones are the most variable in induration. Fine-grained sandstones are generally the most weakly indurated and conglomerates the greatest; however, even with individual units, cementation can vary over distances of decimetres. Crevasse splay deposits of fine sand tend to have more weakly cemented to weakly nodular to blocky induration, although exceptionally permeable horizons may also be well indurated. Fractures in both shales and sandstones have acted as preferential fluid pathways and are therefore more extensively cemented. Fluids appear to have been oxidizing, and the deposition of reduced iron minerals occur as halos surround fossil wood or dinosaur bones indicates. Cements are most commonly carbonate, with some silica, especially in the more indurated units. The concretionary units (Fig. 6) occur within this diagenetic spectrum over a striking distance of at least 11 km.

## Subsurface investigations

Previously, seismic refraction had been carried out on a parallel traverse to the ground penetrating radar (GPR; Shiro & Ferrone 2010). The preliminary work gave encouraging indications that a channel feature could be geophysically mapped into the subsurface. We followed up this work with a GPR survey. Under favourable conditions GPR can provide high-resolution information on sedimentary architecture and has been used to describe the characteristics of other

https://doi.org/10.1017/S1473550411000048 Published online by Cambridge University Press


**Fig. 6.** (a) 5–10 mm concretions weathering out of fine sandstone. (b) Slope mantled by loose concretions. (c) Brown-weathering concretions and vein fill of the same material. (d) Vertical fracture (dashed line) acting as permeability barrier to concretion forming fluids present on right but not left.

Table 3. *XRD analyses of concretions and matrix*

| Sample ID | Material | Quartz (%)* | Calcite (%) | Other% |
|---|---|---|---|---|
| 202 | Concretion | 40 | 60 | None |
| 202 | Matrix | 90 | 10 | None |
| 215 | Concretion | 35 | 65 | None |
| 215 | Matrix | 85 | ND | 10 |
| 295 | ND | 85 | ND | Dickite 15 |
| 439 | Concretion | 25 | 75 | None |
| 459 | Concretion | 60 | 40 | None |
| 463 | Concretion | 60 | 40 | None |

All values are as computed by the JADE™ software and rounded to nearest 5%. Relative accuracy is estimated at 20% of value shown.

Table 4. *PIMA analysis of concretions and matrix*

| Sample | Material | Montmorillonite (%) | Calcite (%) | Other phases detected |
|---|---|---|---|---|
| 215 | Concretion | 39 | 38 | Anhydrite |
| 215 | Concretion | 57 | 43 | |
| 215 | Concretion | 38 | 43 | Anhydrite |
| 215 | Matrix | 64 | 36 | |
| 215 | Matrix | 43 | 34 | Anhydrite |
| 457 | Concretion | 68 | 32 | |
| 457 | Concretion | 67 | 26 | |
| 457 | Concretion | 66 | 29 | |
| 463 | Concretion | 65 | 35 | |
| 463 | Concretion | 72 | 28 | |
| 463 | Concretion | 33 | 32 | Anhydrite |
| 463 | Concretion | 68 | 32 | |

Cretaceous units of the region (cf. Corbeanu *et al.* 2001). We used the CRUX GPR (Kim *et al.* 2006), an instrument developed for future Space Flight Missions, to profile the inferred extension of the KCR palaeochannel beneath the cap of Dakota Formation. This GPR operates at a frequency of 800 Mhz and has a nominal penetration depth of 5 m and a resolution of 15 cm. The instrument was pulled by hand on a small cart. The two GPR profiles clearly show the upper edges of the buried palaeochannel as inverted hyperbola, showing the validity of GPR in delineating such a buried feature (Fig. 5).

### *Concretions*

The concretions are 3–10 mm in diameter, most commonly 5 mm. They are spherical to sub-angular, most commonly

https://doi.org/10.1017/S1473550411000048 Published online by Cambridge University Press

Table 5. *Facies context of concretions*

| Lithology | Structures | Degree of cementation | Concretion abundance | Interpreted environments |
|---|---|---|---|---|
| Conglomerates | Cross-bedding | High | Absent | Very high energy channel |
| Pebbly sandstones | Cross-bedding | Moderate | Less common | High energy channel |
| Medium sandstones | Cross-bedding | Moderate | common | Channel |
| Medium-fine sandstones | Massive to parallel laminated | Moderate | Less common | Splays |
| Fine sandstones | Rippled | Low | Absent | levees |
| Shales | Decimetre-scale bedding | Moderate | Absent | floodplain |

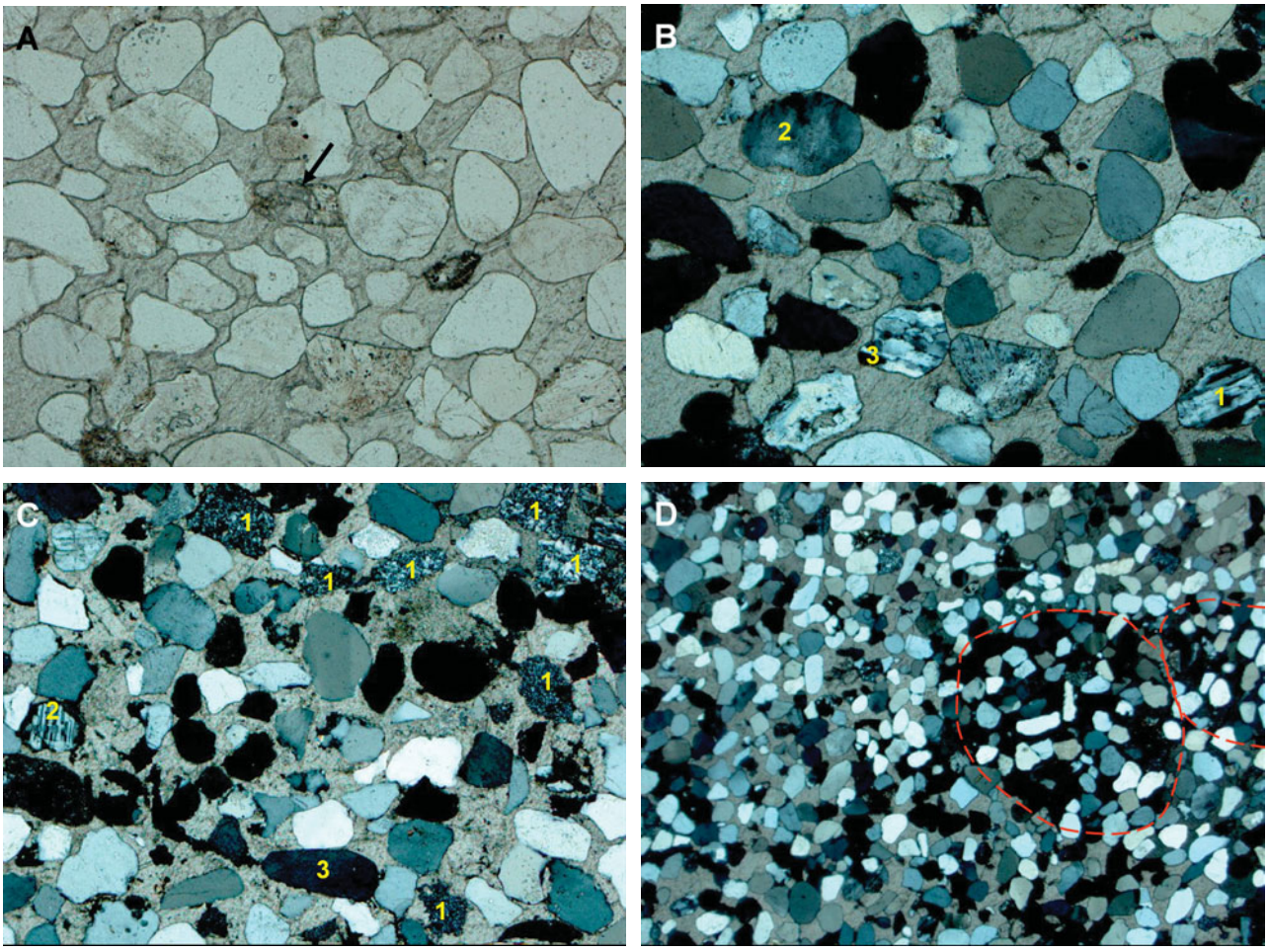


**Fig. 7.** Photomicrographs of concretionary sandstones. (a) Sample 215, plane light, field of view 1.25 mm. Well-rounded sand grains in calcite cement. Calcite-replaced amphibole arrowed. (b) Sample 215, cross-polarized light, field of view 1.25 mm. Grain 1 is plagioclase, grain 2, metamorphic quartz, grain 3 polycrystalline quartz. Other grains, apart from calcite-replaced amphibole in centre, are vein quartz. Poikilotopic calcite cement encloses the grains. (c) Sample 463, cross-polarized light, field of view 1.25 mm. Grains marked 1 are chert, grain 2, plagioclase, grain 4 potassium feldspar (orthoclase). Other grains are vein quartz. Poikilotopic calcite cement encloses the grains. (d) Sample 215, cross-polarized light, field of view 7.8 mm. Circled area of poikilotopic calcite cement undergoing simultaneous extinction. On weathering and surface erosion these domains will form spheroidal concretions.

sub-rounded. Occasional irregular concretions are present. Occasional doublets are formed when two grow close enough to merge, rarely concretions can amalgamate to form multi-nucleate masses. When exposed on a freshly broken surface the concretions are white in colour. They develop a purplish or brown coating on weathering. XRD analysis shows the presence of calcite.

The distribution of the concretions is strongly controlled by depositional facies (Table 2), they are most common in medium-grained channel sandstones, less common in fine-grained or pebbly channel sandstones. Degree and nature of cementation also appears as a factor, concretions occur mostly in moderately indurated sandstones cemented by calcite, they are absent from poorly cemented sandstones and those that have been well cemented by silica.

Distribution of the concretions in the host rocks is not related to individual beds and depositional fabrics, but rather they are more or less evenly spaced. However, on a

https://doi.org/10.1017/S1473550411000048 Published online by Cambridge University Press

Table 6. *Comparison between Brushy Basin Member and Cedar Mountain Formation exhumed and inverted channels*

| Property | Cedar Mountain[1] | Brushy Basin[2] |
|---|---|---|
| Exposed channel length (maximum) | 6.7 km | 3.2 km |
| Width | 17–89 m | 20–100 m |
| Thickness | ~5 m | 2 15–m |
| Lithology | Conglomerates | Medium sands to conglomerates |
| Cement | Carbonate | Carbonate and silica |
| Facies | Migrating meandering channels | Fixed anastomosing channels |
| Age | Early Cretaceous | Late Jurassic |

Sources: [1]Harris (1980), Williams *et al.* (2009).
[2]This paper.

larger scale, some beds contain more than others, and there are patches of concretion-rich sandstone next to concretion-poor sandstone. Early faults act as permeability barriers, with concretions common on one side and not the other (Fig. 6(d)). Similar brown-weathering carbonate occurs in veins (Fig. 6(c)).

Because they are more indurated than the surrounding sandstones, the concretions tend to weather out of the rock. In the process, the surface of the concretions acquires a purplish or brownish colour, suggesting traces of manganese and iron in the carbonate. The liberated concretions are reworked by slope processes to form deposits mantling slopes and as lags within rills and gullies.

### *Mineralogy*

Mineralogy detected by XRD is dominated by quartz and calcite (Table 3), the former presenting the detrital grains in the sandstone, the later the cement. Calcite is more common in the concretions than in the unconcreted sandstone. Dickite and barite were present in XRD traces of two different samples, and these also are probably cement phases.

The PIMA II detected both calcite and montmorillonite in all the samples (Table 4). Anhydrite was detected in several samples, but with lower confidence in identification. Note that the percentages are approximate and are only recorded for the minerals the instrument is able to detect. In the MDRS area, these are carbonates, sulfates and clays. Non-hydrous silicates, such as quartz and feldspar, are not detected.

### *Petrography*

Microscopic examination of the concretionary sandstones shows that they are composed of medium grained, well-rounded and well-sorted sandstones (Table 5). Representative micrographs are shown in Fig. 7.

The sandstones are Quartzose arenites in the classification of Crook (1960). The grains were composed of 95% quartz, including 9% chert, with minor feldspar, both potassium feldspar and plagioclase and clay pellets. There is a trace of amphibole, largely replaced by calcite. The predominantly sedimentary provenance is consistent with a derivation from the folded Palaeozoic rocks to the west (Williams & Hackman 1971).

The cements in the concretions are composed of poikilotopic calcite enclosing multiple sand grains. The staining shows that the calcite is slightly ferroan in some samples. Each crystal is circular to ellipsoidal in cross-section, suggesting that in three dimensions the crystals are spheroids. The crystal size is 3–10 mm, overlapping that of the concretions. We conclude therefore that the concretions are composed of single crystals of calcite. The cement away from the concretions consists of thin clay coatings and minor calcite. The calcite is interpreted as forming during burial.

Clay occurs as grain coatings and cavity fills. Very thin (<10 μm) patchy coatings occur on the sand grains. These are interpreted as forming during or immediately after deposition, and pre-date the main calcite cement. Clay is also present as a fill in irregular cross-cutting vugs in the calcite cement. These vugs are interpreted as forming during dissolution, mostly likely during weathering. This clay generation therefore is of regolith origin possibly derived from the surrounding fine-grained facies.

The petrographic history of the sandstones in these samples therefore consists of the following four events:

1. Deposition.
2. Growth of montmorillonite coatings during shallow burial.
3. Deeper burial, leading to calcite precipitation forming the concretions and minor cements elsewhere.
4. Uplift, exposure and weathering, resulting in vuggy dissolution of the calcite and local infill of the vugs by montmorillonite.

## Inverted and exhumed channel discussion

### *Significance of the channels at the MDRS site*

There have been no previous studies of inverted or exhumed channels from the Brushy Basin Member and previous studies at the MDRS site (e.g. Clarke & Pain 2004; Battler *et al.* 2006) did not refer to them. However, there is an extensive literature on the similar exhumed and inverted channels of the slightly younger Cedar Mountain Formation some 70 km to the north east, near Green River (see Harris 1980; Williams *et al.* 2009 and references therein). The two occurrences are compared in Table 6. Apart from the slightly younger age, the main difference between the two is that the Green River channels are somewhat more continuously exposed and were deposited by meandering rather than anastomosing streams.

### *Mars analogue relevance*

Satellite images of Mars have revealed that numerous inverted and exhumed fluvial channels are present on the Martian surface (e.g. Pain *et al.* 2007; Burr *et al.* 2009; Williams *et al.* 2009; Newsome *et al.* 2010).

Table 7 places the MDRS channels in the context of others that have been discussed as Mars analogues and their Martian counterparts. Inverted and exhumed channels on Mars

https://doi.org/10.1017/S1473550411000048 Published online by Cambridge University Press

Table 7. *Comparisons between different Mars analogue inverted and exhumed channel sites*

| Terrestrial example | Bullengarook[1] | Mirackina[2] | Oman[3] | Robe River[4] | Green River[5] | Hanksville Brushy Basin Member[6] |
|---|---|---|---|---|---|---|
| Morphology | Single fixed channel | Single fixed channel | Distributary meandering channels Distributary braided channels | Single meandering channel | Multiple migrating meandering channels | Multiple fixed anastomosing channels |
| Channel length | >20 km | ~110 km | ~25 and ~45 km | ~130 km | 6.7 km | 3.2 km |
| Width | 1.5–2 km | 50–90 m | 49–108 m 733–1525 m | 500–2000 m | 17–89 m | 20–100 m |
| Thickness | 4 m | 30–40 m | 3–6 m 3.6 m | 80 m | ~5 m | 2–15 m |
| Lithology | Basalt over conglomerate | Sandstone | Cobble conglomerate, pebbly sandstone | Pisolitic ironstone | Conglomerate | Fine sandstone to conglomerate |
| Induration | Basalt infill, silica | Silica | Carbonate | Haematite | Carbonate | Carbonate |
| Mars example | Juventae Chasma[7] | Miyamoto[8] | Eberswalde[9] and Aeolis[10] fans | Arabia[11] | Eberswalde fan[9] | Aeolis channels[10] |

Sources: [1] Ollier & Pain (1995), Pain *et al.* (2007).
[2] McNally & Wilson (1995), Pain *et al.* (2007).
[3] Miazels 1987, Burr *et al.* (2009).
[4] Morris & Ramanaidou (2007), Heim *et al.* (2006).
[5] Harris (1980), Williams *et al.* (2009).
[6] This paper.
[7] Lucchitta (2005).
[8] Newsome *et al.* (2010).
[9] Bhattacharya *et al.* (2005).
[10] Burr *et al.* (2009).
[11] Pain *et al.* (2007).

markedly different in morphology, including basalt (Lucchitta 2005) and sediment-filled (e.g. Bhattacharya *et al.* 2005), single (Pain *et al.* 2007; Newsome *et al.* 2010) and anastomosing channels (Burr *et al.* 2009), fans and deltas (Bhattacharya *et al.* 2005; Pain *et al.* 2007; Burr *et al.* 2009), and fixed (Newsome *et al.* 2010) and migrating high-sinuosity (Bhattacharya *et al.* 2005) channels. Therefore, a diversity of terrestrial analogues is needed.

As anastomosing fixed channels, the MDRS examples, although segmented, are among the best terrestrial analogues yet identified for those of the Aeolis region on Mars (Burr *et al.* 2009), as illustrated in Fig. 8. The complex terrain and segmentation of the exhumed and inverted channels at the MDRS site also provide superb exposure and access to study the detailed fluvial architecture.

Finally, although we did not investigate this aspect of the MDRS palaeochannels, some examples elsewhere in the world contained well-preserved microfossils and, when inverted and exhumed channels provide excellent sampling sites (Macphail & Stone 2004). Exhumed and inverted channels on Mars can also be expected to host such remains, if they exist. Terrestrial palaeochannels have also provided refugia for biota as climates shift from equitable to more arid over timescales of tens of millions of years and formerly surface organisms adapt to habitats in the sedimentary pores (Macphail & Stone 2004; Finston *et al.* 2007).

## Concretion discussion

### *Significance of the concretions at MDRS*

As Clifton (1957) aptly put it: 'The origin of concretions is a geologic puzzle'. Their origin is often obscure and the evidence from them contradictory (Selles-Martinez 1996). However, a detailed analysis of their context, fabric, mineralogy and chemistry allows some conclusions to be drawn about their formation and significance.

We infer that the distribution of concretions in Brushy Basin Member at the MDRS field site is strongly controlled by the hydrology that in turn is controlled by the depositional architecture. More work is needed in this field to map out the extent of the concretions.

The timing of the concretions is therefore interpreted as occurring during burial, subsequent to early cementation and early fracturing, but prior to final infill of porosity by cement. More work is needed, in particular petrographic studies, to determine the relative timing relationships.

### *Mars analogue value*

Vast numbers of small spherical haematite concretions are a striking feature of the Burns formation at Meridiani Planum seen by the *Opportunity* rover (Klingelhofer *et al.* 2004; McLennan *et al.* 2005; Sefton-Nash & Catling 2008). A number of terrestrial examples are proposed as analogues,

https://doi.org/10.1017/S1473550411000048 Published online by Cambridge University Press

Table 8. *Comparisons between different Mars analogue concretion sites*

| Property | Meridiani[1] | Navajo Sandstone Concretions[2] | WA concretions[3] | Mauna Kea concretions[4] | Hanksville Dakota Concretions[5] | Hanksville Brushy Basin Concretions[6] |
|---|---|---|---|---|---|---|
| Host texture | Sand | Sand | Sand | Breccia | Sand | Sand |
| Host mineralogy | Altered basalt, sulfates | Quartz | Quartz, sulfates | Altered basalt | Quartz | Quartz |
| Host facies | Saline lakes and associated dunes | Dune sands | Saline lakes | Cinder cone | Marginal marine sands | Fluvial channels |
| Concretion mineralogy | Haematite | Haematite | Haematite | Haematite | Goethite | Calcite |
| Concretion sphericity | Moderate-high | Low to high | Low-moderate | High | Moderate | Moderate-high |
| Concretion dimensions | 1–8 mm (most 2–5) | 1–100 mm | 100 μm–10 mm | 30–40 μm | 5–10 mm | 3–10 (most 5) |
| Concretion fabric | Homogeneous to concentric | Homogeneous to concentric | Homogeneous to concentric | Homogeneous-rimmed | Poikilotopic | Poikilotopic |
| Weathering properties | Weather out | Weather out | Do not weather out | Do not weather out | Do not weather out | Weather out |
| Extent | 10s of km | km | km | < 1 km | 10s of km? | 10s of km? |
| Greatest analogue value | | Mineralogy, fabric, host facies, surface expression | Mineralogy, host lithology, host facies | Mineralogy, host lithology | Extent | Extent, sphericity, surface expression |

Sources: [1]Klingelhofer *et al.* (2004) and McLennan *et al.* (2005).
[2]Chan *et al.* (2004).
[3]Benison & Bowen (2006) and Benison *et al.* (2007).
[4]Morris *et al.* (2005).
[5]Battler *et al.* (2006).
[6]This paper.

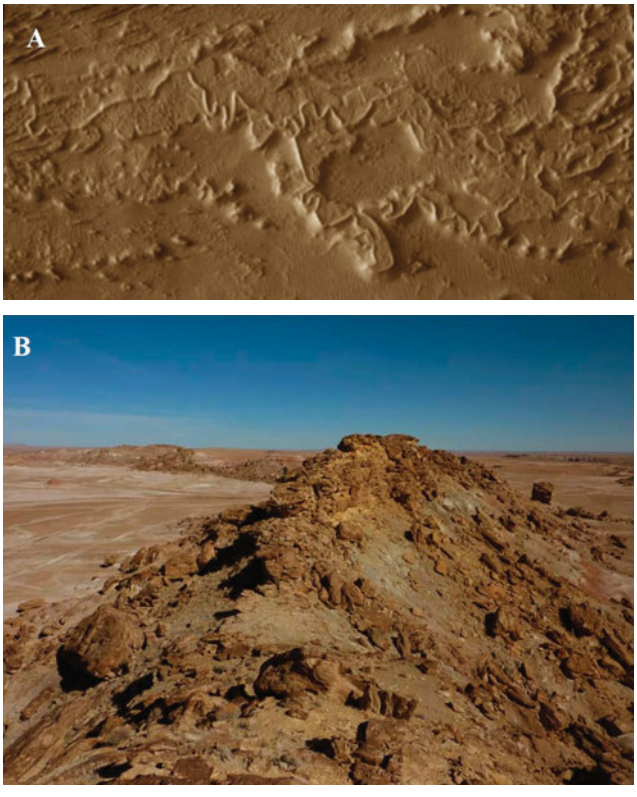


**Fig. 8.** Comparison of terrestrial and Martian channels. (A) Inferred anastomosing fixed channels in Aeolis, from Themis Image V05875001. (B) Fifty-metre high silicifed fixed anastomosing channel of KCR, MDRS site.

most notably those from the Aeolian Navajo Sandstone (Chan *et al.* 2004), altered volcanic breccia at Mauna Kea (Morris *et al.* 2005), Western Australian salt lakes (Benison & Bowen 2006; Benison *et al.* 2007) and the marginal marine sandstones in the Dakota Formation at MDRS (Battler *et al.* 2006). As with all analogues, these examples have both similarities and differences to the Martian feature they are intended to counterpart. Table 8 shows these similarities and differences with respect to host rock texture, mineralogy and facies, along with concretion mineralogy, sphericity, texture, dimensions and extent. From Table 8 the best analogues are those in the Navajo Sandstone, followed by those in the WA salt lake concretions, Brushy Basin Member and Dakota Sandstone, with the Moana Kea concretions last.

With regard to host rock textures, the Navajo, WA, Dakota and Brushy Basin provide the best analogues, all occurring in sands. Regarding host mineralogy the WA and Moana Kea are the best, each individually reflecting one aspect of the main compositional lithologies at Meridiani, sulfates and altered basalt, respectively. The combined Aeolian and salt lake depositional environment at Meridiani are best represented by the end member analogues on Earth, with the Navajo concretions forming in dune sands and the WA concretions in acidic sulfate-rich salt lakes. The Meridiani haematite mineralogy is best reflected by the Navajo and WA concretions. Morphologically, the Brushy Basin concretions are the most similar in sphericity and size. With respect to internal fabric the Navajo concretions show the greatest similarities being internally homogeneous to concentric, this is shared by

https://doi.org/10.1017/S1473550411000048 Published online by Cambridge University Press

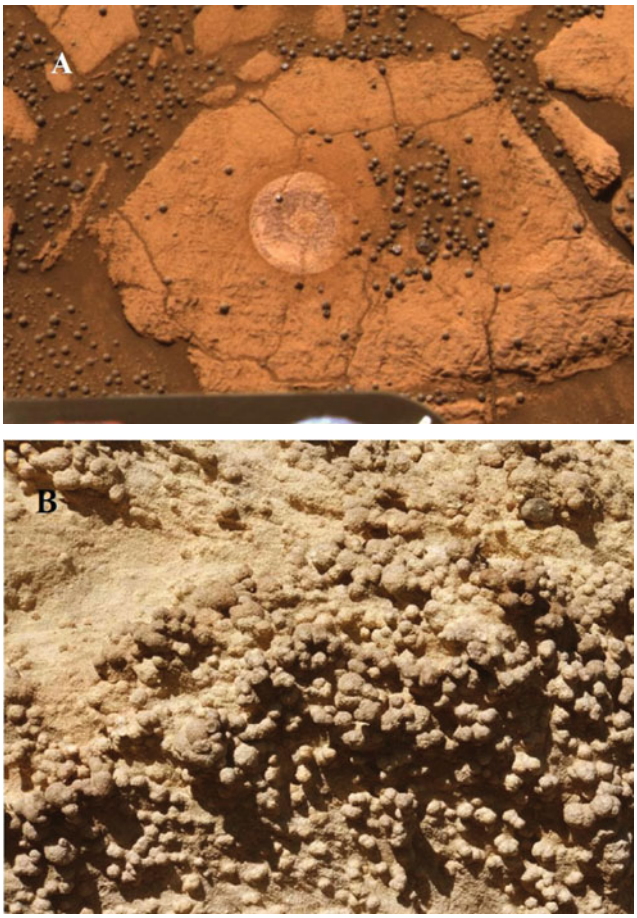


**Fig. 9.** (a) *In situ* and remobilized concretions at 'Berry bowl' location (Eagle Crater), Meridiani Planum (NASA image). (b) *In situ* concretions on side of KCR, diameter 5–10 mm.

some of the Moana Kea and WA concretions. Dimensionally, the concretions of the Brushy Basin Member mostly resemble those of Meridiani. In terms of extent, both the Dakota and Bushy Basin concretionary units resemble those on Mars in extending for at least 10 km laterally. Lastly, in terms of geomorphic behaviour, both the Navajo and Brushy Basin concretions are significantly harder than their host rocks and weather out in a manner analogous to those on Mars.

Which of these analogues are the best therefore depends on the property being investigated. The Navajo concretions are the best with regard to mineralogy and fabric and share with the WA examples a similarity in depositional environment. The WA concretions are the only ones associated with sulfates and the Moana Kea with basaltic volcanics. The concretions in the Brushy Basin Member are, however, the best analogues in terms of their extent, sphericity and surface expression (Fig. 9).

Only haematite concretions have been found on Mars to date. However, the detection of carbonate in deltaic sediments in Jerezo Crater (Murchie *et al.* 2009) hints at carbonate-overprinted of sediments on the planet, at least locally. Whether the carbonate in the Jerezo Crater palaeochannels occurs as distributed cement, weathering-related overprint or as discrete concretions, as is the case of the Brushy Basin Member concretions at the MDRS field site, remains to be seen. However, the presence of relatively abundant carbonate overprints in the hydrothermal altered volcanics of Comanche Spur rocks in Gusev Crater on Mars (Morris *et al.* 2010) indicates that abundance of secondary carbonate at least locally on Mars. Thus, the carbonate cements and concretions at MDRS can be taken as illustrating at least some of the characteristics of diagenetic carbonates in rocks otherwise dominated by weathered and altered volcanic products and detrital grains.

## Astrobiological applications and implications

A key part of assessing the astrobiological potential of a site requires knowledge of the history of water activity. This information is encoded in the depositional and diagenetic history. Well-exposed features such as inverted palaeochannels provide opportunities to access the exposures to acquire such information as depositional environment, water density drying deposition and subsequent fluid history. In addition, terrestrial-inverted channels are also excellent locations to find fossils (Macphail & Stone 2004) and can provide subsurface refugia to surface biota driven underground by increasing aridity (Finston *et al.* 2007). Terrestrial inverted and exhumed palaeochannels therefore also provide targets for astrobiological research and the development of technologies and methodologies to look for fossils on Mars in such features.

## Lessons for future exploration

Understanding of such features is important as they occur in sites proposed as targets for future missions such as Mars Science Laboratory (*Curiosity*) (Marzo *et al.* 2009; Rice & Bell 2010) and they contain a wealth of information about Martian processes including fluvial hydrology, water chemistry, fluid flow and constraining landscape evolution. However, exhumed and inverted channels typically have steep-sided exposures, often covered in rubbly deposits, making access difficult (Fig. 10). Astronauts, even though hampered by pressure suits, may well find it easier to traverse such slopes than autonomous or remotely controlled vehicles. However, un-exhumed channels may be more easily accessed provided they can be located by geophysical means.

We have also shown that geophysical techniques, specially GPR are able to locate such channels in the subsurface, at least when adjacent to known exposures, allowing access from above using drills, if required. Although avoiding the problems of traversing difficult terrain, field experience (Shiro & Ferrone 2010) has shown that the handling and deployment of such complex instruments and tools will likewise be greatly facilitated by direct human presence.

## Future work

Investigations of the site are continuing. These include analysis of textures and materials recovered from drill core,

https://doi.org/10.1017/S1473550411000048 Published online by Cambridge University Press

**Fig. 10.** Typical difficult terrain making up inverted and exhumed channels. Photo courtesy: Line Drube.

petrography of thin sections and further examination of the mineralogy of sediments, concretions and soils using both XRD and infrared spectroscopy. We expect these studies to reveal further details of the diagenesis and fluid history of these sediments and their relevance to Mars analogue studies. We also hope to revisit the site and map out the extent of the concretions in locations at greater distances from MDRS.

## Conclusions

We conclude that the inverted relief at MDRS is an excellent example of some types of inverted and exhumed relief at Mars. They are particularly close analogues to the inverted anastomosing channels of Aeolis. Studying the MDRS channels assists in understanding the processes of sedimentation and landscape evolution that shape such features, predicts the detailed features that will be encountered when they are explored at ground level by future Mars missions, and provide testing grounds for the technology and instrumentation required for their study.

The Concretions at MDRS are a partial analogue to concretions discovered at Meridiani on Mars by the *Opportunity* rover. They are particularly good analogues with respect to size, shape, distribution, extent and in their geomorphic expression as they weather out of the substrate and concentrated as surface lags.

Lastly, we emphasize that the area surrounding MDRS has considerable Mars analogue value, the presence of the concretions and inverted and exhumed channels adds to a diverse suite of analogues that includes sulfate soils, bedded sulfate evaporites and gullies. All these features occur in close proximity to the station itself, which are designed and equipped to simulate many of the aspects of a Mars station. The area is an ideal location for both specialized and highly integrated studies of Mars analogues and their exploration.

## Acknowledgements

This project was funded through the NASA Moon and Mars Analogs programme. We thank the US Mars Society for allowing us to use the facilities at MDRS, especially Artemis Westenberg, the facility project manager. MDRS crews 89 and 92 provided essential support and assistance in the field. These crews were supported by the International Lunar Exploration Working Group (ILEWG), the European Space Research and Technology Centre (ESTEC) and the Ecole de l'Air as part of EuroMoonMars campaign. The CRUX GPR was loaned to us by Soon Sam Kim. The XRD analysis was performed using a Terra XRD on loan from David Blake, who also assisted with interpretation of the data. Geoscience Australia provided the PIMA facilities. Lastly, we thank the efforts of the anonymous reviewers whose input was of great value in the preparation of the paper.

## References

Battler, M.M., Clarke, J.D.A. & Coniglio, M. (2006). Possible analog sedimentary and diagenetic features for Meridiani Planum sediments near Hanksville, Utah: implications for Martian field studies. In *Mars Analog Research*, ed. Clarke, J.D.A., pp. 55–70. American Astronautical Society Science and Technology Series 111. Univvelt Inc, San Diego, California.

Benison, K.C. & Bowen, B.B. (2006). Acid saline lake systems give clues about past environments and the search for life on Mars. *Icarus* **183**, 225–229.

Benison, K.C., Bowen, B.B., Oboh-Ikuenobe, F.E., Jagniecki, E.A., Laclair, D.A., Story, S.L., Mormile, R.M. & Hong, B.-Y. (2007). Sedimentology of acid saline lakes in southern Western Australia: newly

https://doi.org/10.1017/S1473550411000048 Published online by Cambridge University Press

described processes and products of an extreme environment. *J. Sediment. Res.* **77**, 366–388.

Bhattacharya, J.P., Payenberg, T.H.D., Lang, S.C. & Bourke, M. (2005). Dynamic river channels suggest a long-lived Noachian crater lake on Mars. *Geophys. Res. Lett.* **32**, L10201. doi:10.1029/2005GL022747.

Burr, D.M., Enga, M.T., Williams, R.M.E., Zimbelman, J.R., Howard, A.D. & Brennan, T.A. (2009). Pervasive aqueous paleoflow features in the Aeolis/Zephyria Plana region, Mars. *Icarus* **200**, 52–76.

Chan, M.A., Beitler, B., Parry, W.T., Ornö, J. & Komatsu, G. (2004). A possible terrestrial analogue for haematite concretions on Mars. *Nature* **429**, 731–734.

Clarke, J.D.A. & Pain, C.F. (2004). From Utah to Mars: regolith-landform mapping and its application. In *Mars Expedition Planning*, ed. Cockell, C.C., pp. 131–160. American Astronautical Society Science and Technology Series 107.

Clifton, H.E. (1957). The carbonate concretions of the Ohio shale. *Ohio J. Sci.* **57**, 114–124. Univvelt Inc, San Diego, California.

Corbeanu, R.M., Wizevich, M.C., Bhattacharya, J.P., Zeng, X. & McMechan, G.A. (2001). Three-dimensional architecture of ancient lower delta-plain point bars using ground-penetrating radar, Cretaceous Ferron Sandstone, Utah. *AAPG Stud. Geol.* **50**, 427–449.

Crook, K.A.W. (1960). Classification of arenites. *Am. J. Sci.* **258**, 419–428.

Demko, T.M., Currie, B.S. & Nicoll, K.A. (2004). Regional paleoclimatic and stratigraphic implications of paleosols and fluvial/overbank architecture in the Morrison formation (Upper Jurassic), Western Interior, USA. *Sediment. Geol.* **167**, 115–135.

Demko, T.M. & Parish, J.T. (2001). Paleoclimatic setting of the Upper Jurassic Morrison formation. *Mod. Geol.* **22**, 283–296.

Finston, T.L., Johnson, M.S., Humphreys, W.F., Eberhard, S.M. & Halse, S.A. (2007). Cryptic speciation in two widespread subterranean amphipod genera reflects historical drainage patterns in an ancient landscape. *Mol. Ecol.* **16**, 355–365.

Foing, B., Stoker, C., Zavaleta, J., Ehrenfreund, P., Thiel, C., Sarrazin, P., Blake, D., Page, J., Pletser, V., Hendrikse, J. *et al.* (2011). Field astrobiology research in Moon–Mars analogue environment: instruments and methods. *Int. J. Astrobiol.* **10**, 141–160.

Harris, D.R. (1980). Exhumed paleochannels in the Lower Cretaceous Cedar Mountain formation near Green river. *Utah*: *Brigham Young Univ. Geol. Stud*. **27**, 51–66.

Heim, J.A., Vasconcelos, P.M., Shuster, D.L., Farley, K.A. & Broadbent, G. (2006). Dating paleochannel iron ore by (U-Th)/He analysis of supergene goethite, Hamersley province, Australia. *Geology* **34**(3), 173–176.

Hintze, L.H. & Kowallis, B.J. (2009). *The Geologic History of Utah Brigham*. Young University Geology Studies Special Publication 9. Department of Geology, Brigham Young University, Provo, Utah, 202 p.

Howard, A.D., Moore, J.M. & Irwin, R.P. (2005). An intense terminal epoch of widespread fluvial activity on early Mars: 1. Valley network incision and associated deposits. *J. Geophys. Res.* **110**(E12S14), doi:10.1029/2005JE002459.

Irwin, R.P., Howard, A.D. III, Craddock, R.A. & Moore, J.M. (2005). An intense terminal epoch of widespread fluvial activity on early Mars: 2. Increased runoff and paleolake development. *J. Geophys. Res.* **110**(E12S15), doi:10.1029/2005JE002460.

Kim, S.S., Carnes, S.R., Haldemann, A.F., Ulmer, C.T., Ng, E. & Arcone, S.A. (2006). Miniature Ground Penetrating Radar, CRUX GPR. Presentation to IEEE Aerospace Conference, Big Sky, Montana, 6–9 March 2006. http://trs-new.jpl.nasa.gov/dspace/bitstream/2014/38905/1/06-0566.pdf

Kjemperud, A.V., Schomacker, E.R. & Cross, T.A. (2008). Architecture and stratigraphy of alluvial deposits, Morrison formation (Upper Jurassic), Utah. *AAPG Bull.* **92**(8), 1055–1076.

Klingelhofer, G., Morris, R.V., Bernhardt, B., Schröder, C., Rodionov, D.S., de Souza, P.A., Yen, A., Gellert, R., Evlanov, E.N., Zubkov, B. *et al.* (2004). Jarosite and hematite at Meridiani Planum form Mossbauer spectrometer on the Opportunity rover. *Science* **306**, 1740–1745.

Lucchitta, B.K. (2005). Light layer and sinuous ridges on plateau near Juventae Chasma, Mars. In Abstracts of the 36th Lunar and Planetary Science Conference, Abstract 1500.

Macphail, M.K. & Stone, M.S. (2004). Age and palaeoenvironmental constraints on the genesis of the Yandi channel iron deposits, Marillana formation, Pilbara, northwestern Australia. *Aust. J. Earth Sci.* **51**, 497–520.

Mangold, N., Ansan, V., Masson, P., Quantin, C. & Neukum, G. (2008). Geomorphic study of fluvial landforms on the northern Valles Marineris plateau, Mars. *J. Geophys. Res.* **113**(E08009), doi:10.1029/2007JE002985.

Marzo, G.A., Oush, T.L., Lanza, N.L., McGuire, P.C., Newso, H.E., Olilla, A.M. & Wiseman, S.M. (2009). Mineralogy of the inverted channel on the floor of Miyamoto Crater, Mars. In Abstracts 40th Lunar and Planetary Science Conference, abstract 1236.

McLennan, S.M., Bell, J.F., Calvin, W.M., Christensen, P.R., Clark, B.C., de Souza, P.A., Farmer, J., Farrand, W.H., Fike, D.A., Gellert, R. *et al.* (2005). Provenance and diagenesis of the evaporite-bearing Burns formation, Meridiani Planum, Mars. *Earth Planet. Sci. Lett.* **240**, 95–121.

McNally, H.H. & Wilson, I.R. (1995). Silcretes of the Mirackina Palaeochannel, Arckaringa, South Australia. *AGSO J. Austr. Geol. Geophys.* **16**, 295–301.

Miall, A.E. & Turner-Peterson, C. (1989). Variations in fluvial style in Westwater canyon Member, Morrison formation (Jurassic), San Juan Basin, Colorado Plateau. *Sediment. Geol.* **63**, 21–60.

Miazels, J.K. (1987). Plio-Pleistocene raised channel systems of the western Sharqiya (Wahiba), Oman. *Geological Society, London, Special Publications* **35**, 31–50.

Morris, R.V., Ming, D.W., Graff, T.G., Arvidson, R.E., Bell, J.F., Squyres, S.W., Mertzman, S.A., Gruener, J.E., Golden, D.C., Le, L. *et al.* (2005). Hematite spherules in basaltic tephra altered under aqueous, acid-sulfate conditions on Mauna Kea volcano, Hawaii: possible clues for the occurrence of hematite-rich spherules in the Burns formation at Meridiani Planum, Mars. *Earth Planet. Sci. Lett.* **240**, 168–178.

Morris, R.C. & Ramanaidou, E.R. (2007). Genesis of the channel iron deposits (CID) of the Pilbara region, Western Australia'. *Aust. J. Earth Sci.* **54**(5), 733–756.

Morris, R.V., Ruff, S.W., Gellert, R., Ming, D.W., Arvidson, R.E., Clark, B.C., Golden, D.C., Siebach, K., Klingelhöfer, G., Schröder, C. *et al.* (2010). Identification of carbonate-rich outcrops on Mars by the Spirit Rover. *Science* **239**, 421–424. DOI: 10.1126/science.1189667.

Murchie, S.L., Mustard, J.F., Ehlmann, B.L., Milliken, R.E., Bishop, J.L., McKeown, N.K., Dobrea, E.Z.N., Seelos, F.P., Buczkowski, D.L., Wiseman, S.M. *et al.* (2009). A synthesis of Martian aqueous mineralogy after 1 Mars year of observations from the Mars Reconnaissance Orbiter. *J. Geophys. Res.* **114**(E00D06), doi:10.1029/2009JE003342.

Newsome, N.E., Lanza, N.L., Ollila, A.M., Wiseman, S.M., Roush, T.L., Marzo, G.A., Tornabene, L.L., Okubo, C.H., Osterloo, M.M., Hamilton, V.E. *et al.* (2010). Inverted channel deposits on the floor of Miyamoto crater, Mars. *Icarus* **205**, 64–72.

Pain, C.F., Clarke, J.D.A. & Thomas, M. (2007). Inversion of relief on Mars. *Icarus* **190**, 478–491.

Pain, C.F. & Ollier, C.D. (1995). Inversion of relief – a component of landscape evolution. *Geomorphology* **12**(2), 151–165.

Persaud, R., Rupert-Robles, S., Clarke, J.D.A., Dawson, S., Mann, G., Waldie, J., Piechocinski, S. & Roesch, J. (2004). Expedition one: a Mars analog research station thirty-day mission. In *Mars Expedition Planning*, ed. Cockell, C.C., pp. 53–88. American Astronautical Society Science and Technology Series 107. Univvelt Inc, San Diego, California.

Rice, M.S. & Bell, J.F. (2010). Geologic mapping of the proposed Mars Science Laboratory (MSL) landing ellipse in Eberswalde Crater. In Abstracts 41st Lunar and Planetary Science Conference, Abstract 2524.

Sarrazin, P., Blake, D., Feldman, S., Chipera, S., Vaniman, D. & Bish, D. (2005). Field deployment of a portable X-ray diffraction/X-ray fluorescence instrument on Mars analog terrain. *Powder Diffr.* **20**(2), 128–133.

Sefton-Nash, E. & Catling, D.C. (2008). Hematitic concretions at Meridiani Planum, Mars: their growth timescale and possible relationship with iron sulfates. *Earth Planet. Sci. Lett.*. **269**, 365–375.

Selles-Martinez, J. (1996). Concretion morphology, classification and genesis. *Earth Sci. Rev.* **41**, 177–210.

Shiro, B.R. & Ferrone, K.L. (2010). *In situ* geophysical exploration by humans in Mars analog environments. In Abstracts 41st Lunar and Planetary Science Conference, Abstract 2052.

Soderblom, L.A., Anderson, R.C., Arvidson, R.E., Bell, J.F., Cabrol, N.A., Calvin, W., Christensen, P.R., Clark, B.C., Economou, T., Ehlmann, B.L. *et al.* (2004). The soils of Eagle crater and Meridiani Planum. *Science* **306**, 1723–1726.

Stoker, C.R., Clarke, J., Direito, S., Martin, K., Zavaleta, J., Blake, D. & Foing, F. (2011). Chemical, mineralogical, organic and microbial properties of subsurface soil cores from the Mars Desert Research Station Utah: analog science for human missions on Mars. *Int. J. Astrobiol.* **10**, 269–289.

Thomas, M. & Walter, M.R. (2002). Application of hyperspectral infrared analysis of hydrothermal alteration on Earth and Mars. *Astrobiology* **2**(3), 335–351.

Western Regional Climate Center (2010). Climate Data for Hanksville Utah. http://www.wrcc.dri.edu/cgi-bin/cliMAIN.pl?uthank

Williams, P.L. & Hackman, R.J. (1971). Geology of the Salina quadrangle, Utah. United States Geological Survey Miscellaneous Geological Investigations 1:250,000 scale geological map I-591-A., Department of the Interior.

Williams, R.M.E., Irwin, R.P. & Zimbelman, J.R. (2009). Evaluation of paleohydrologic models for terrestrial inverted channels: Implications for application to Martian sinuous ridges. *Geomorphology* **107**, 300–315.

https://doi.org/10.1017/S1473550411000048 Published online by Cambridge University Press